Available online at www.sciencedirect.com
SCIENCE DIRECT®
International Journal of Mass Spectrometry 232 (2004) 171–183
International Journal of Mass Spectrometry
www.elsevier.com/locate/ijms

# A fragmentation study of an isoflavone glycoside, genistein-7-*O*-glucoside, using electrospray quadrupole time-of-flight mass spectrometry at high mass resolution

Raymond E. March [a,b,*], Xiu-Sheng Miao [b], Chris D. Metcalfe [b], Maciej Stobiecki [c], Lukasz Marczak [c]

[a] *Department of Chemistry, Trent University, 1600 West Bank Drive, Peterborough, Ont., Canada K9J 7B8*
[b] *Water Quality Centre, Trent University, 1600 West Bank Drive, Peterborough, Ont., Canada K9J 7B8*
[c] *Institute of Bioorganic Chemistry, Polish Academy of Science, Noskowskiego 12/14, 61-702 Poznan, Poland*

Received 23 September 2003; accepted 7 January 2004

**Abstract**

A mass spectrometric method based on the combined use of electrospray ionization, collision-induced dissociation and tandem mass spectrometry at high mass resolution has been applied to an investigation of the structural characterization of genistein-7-*O*-β-D-glucoside (5,7,4′-trihydroxyisoflavone). The product ion mass spectrum of $[M-H]^-$ ions shows neutral losses of the glycan residue (162 Da) and of the glycan residue + H• (163 Da) by rearrangement and scission, respectively, where the latter loss dominates at higher collision energies. The genistein moiety remained intact and only minor fragmentation of the glucose moiety was observed. The low-energy product ion mass spectrum of $[M+H]^+$ ions shows extensive fragmentation of the glucose moiety, though at low ion signal intensity, loss of the glycan residue, and simple fragmentation of the genistein moiety that permits characterization of the substituents in the A and B rings. The use of elevated cone voltages permitted observation of product ion mass spectra of selected primary fragment ions. Product ion mass spectra examined at high mass resolution allowed unambiguous determination of the elemental composition of fragment ions. Fragmentation mechanisms and ion structures have been proposed.


*Keywords:* Genistein-7-*O*-glucoside; Tandem mass spectrometry; Flavonoid glycoside; Accurate mass; Electrospray ionization

## 1. Introduction

The study of the class of phytochemicals known as the flavonoids has been confined largely heretofore to their distribution in the plant kingdom, elucidation of their structures, and the pathways by which they are synthesized. Flavonoid is a collective noun given to several classes of structurally similar, plant secondary metabolites; the major classes are flavones, isoflavones, flavans, anthocyanins, proanthcyanidins, flavanones, chalcones, and aurones. The flavonoids were reviewed extensively in 1994 [1]. Plants synthesize flavonoids along with other secondary metabolites for protection against pathogens and herbivores. Flavonoids are ubiquitous in the environment; they are found primarily in petals, the foliage of trees and bushes, and are widely distributed in the edible parts of plants.

Flavonoids and isoflavonoids may be of ecotoxicological importance since they are present in the heartwood of tree species used for wood pulp [2,3] and are to be found in a variety of fruits and vegetables. Plants of the Leguminosae family (e.g. soy, lupin) contain isoflavones that are important components of the diets of humans and animals. Flavonoids are of environmental significance because several flavonoid aglycones (flavonoid glycosides that have lost the sugar moiety) are known to be biologically active [4] while some isoflavones are also phytoestrogens [5,6] that have radical scavenger [7,8] and anticarcinogenic [9,10] activities. While phytochemicals in the heartwood and sapwood of trees render the wood resistant to disease [2], flavonoids in mammals can affect reproduction by acting upon the pituitary–gonadal axis, either as competitors for steroid receptor sites [11] or by inhibiting aromatase [12]. Flavonoids are present also in

* Corresponding author. Tel.: +1-705-748-1011x5886; fax: +1-705-748-1625.
*E-mail address:* rmarch@trentu.ca (R.E. March).

1387-3806/$ – see front matter © 2004 Elsevier B.V. All rights reserved.
doi:10.1016/j.ijms.2004.01.001

herbal medicines [13] and preventative therapeutics [9]. The potential health effects of flavonoids demand that methods be developed for their determination and quantification in food products, plant extracts, and serum.

The advent of fast atom bombardment (FAB), atmospheric pressure chemical ionization (APCI), and electrospray ionization (ESI) combined with tandem mass spectrometry (MS/MS) has permitted ready study of the flavonoids, their ion chemistry, and the determination of flavonoids in low concentrations in aqueous systems. Mass spectrometric methods coupled to liquid chromatography show great promise for the analysis and quantification of these compounds in biological samples [14–17], food products [18], plant extracts [19–21], and for fundamental studies [22–29]. Thermospray LC/MS/MS has been used for the characterization of flavonoids [30] and the rapid screening of fermentation broths for flavones [31]. Using ion spray LC/MS/MS, parent ion scans of the two protonated aglycones, quercitin and kaempferol, indicated the presence of more than 12 different flavonol glycosides among nine hop varieties [32]. Ion spray LC/MS/MS has been used also for the characterization of flavonoids in extracts from *Passiflora incarnata* [33,34]. APCI/MS/MS has been employed for the quantitative analysis of xanthohumol and related prenylflavonoids in hops and beer [35], for a study of flavonone absorption following naringin, hesperidin, and citrus administration [36] and for the identification of 26 aglycones from the leaf surfaces of *Chrysothamnus* [37]. ESI/MS/MS has been employed for the investigation of 14 flavonoids [38], apigenin anionic clusters in the gas phase [39], $Na^+$-bound clusters of quercetin in the gas phase [40], flavonoid aglycones [41], and characterization of flavonoid *O*-diglycosides [42,43]. The combination of MS/MS with these ionization techniques for polar compounds has proven to be a valuable technique that has great sensitivity, specificity, mass range, and mass resolution.

Genistein-7-*O*-β-D-glucoside (5,7,4′-trihydroxyisoflavone) was selected for this study because of its wide range of biological activities both in plant physiology and biochemistry [7,44], its estrogenic effect on women [5,6], and anticarcinogenic properties [10]. Genistein is present in wood pulp and in treated and untreated pulp mill effluents, and it is probable that genistein and possibly other flavonoids are present in the receiving waters of pulp mills [38]. The investigation of genistein-7-*O*-glucoside forms a necessary base-line study for our current examination of flavonoids and flavonoid glycosides [38–40,45]. This fragmentation study of genistein-7-*O*-glucoside consists of an examination of the fragmentation of protonated genistein-7-*O*-glucoside and of deprotonated genistein-7-*O*-glucoside formed by ESI. The mass/charge ratios of the fragment ions were obtained at high mass resolution to within 0.1 mDa. Pathways for the formation of primary fragment ions are proposed. For the observation of product ion mass spectra of primary fragment ions, signal ion intensities of primary fragment ions were maximized by variation of the cone voltage. Fragment ions generated at elevated cone voltages upstream of the first mass-resolving element can be subjected to CID so as to identify direct product ion–precursor ion relationships. The utilization of enhanced cone voltage to maximize first generation fragment ion signal intensity can yield pseudo-MS/MS/MS performance in the Q-TOF II™ mass spectrometer that is useful in determining the hierarchy of fragment ions. In the examination of a standard substance such as genistein-7-*O*-glucoside, the probability of isolating more than one isobaric fragment ion species in the first quadrupole mass filter is zero when such ions are not detected in the initial product ion mass spectrum.

Each of the primary ion species obtained thus was isolated in the mass-resolving quadrupole mass filter and fragmented further in the collision cell. This process of examination of primary, secondary, and tertiary ions was continued until prevented by lack of ion signal intensity. While the measurement of precise mass/charge ratios of fragment ions of low mass/charge ratio were difficult due to low signal ion intensity, each fragment ion reported was observed as a direct product of its immediate precursor ion. Ion structures have been proposed for each of the fragments observed in the fragmentation of the $(Y_o - H)^{\bullet -}$ ion of *m*/*z* 268.

## 2. Experimental

### 2.1. Materials

Genistein-7-*O*-glucoside was purchased from Sigma Chemical Co. (St. Louis, MO, USA). Methanol was purchased from Fisher (Fair Lawn, NJ, USA). The analyte solution was prepared using methanol and water (1:1) at a concentration of 100 μg ml$^{-1}$. The solution was infused to the ESI source using a Harvard Apparatus Model 11 syringe pump (Harvard Apparatus, Holliston, MA, USA) at a flow rate of 10 μl min$^{-1}$.

### 2.2. ES mass spectrometry

ES mass spectrometry and MS/MS experiments were performed on a Q-TOF 2™ mass spectrometer with a Z-spray™ ES source (Micromass, Manchester, UK). The ES source potentials were: capillary 3.0 kV and extractor 2 V. The sampling cone voltage was varied from 20 to 140 V for ES mass spectra and the specific value of the cone voltage for each collision-induced dissociation (CID) experiment is given in the text. The quadrupole mass filter to the TOF analyzer was set with LM and HM resolution of 15.0 (arbitrary units), which is equivalent to a 1.0 Da mass window for transmission of precursor ions. The source block and desolvation temperatures were set at 80 and 150 °C, respectively. All single analyzer mass spectra were obtained by scanning the TOF analyzer. CID of mass-selected ions was performed in an rf-only quadrupole collision cell. Ultra-high purity (UHP) argon was used as the collision

gas at 10 psi inlet pressure for CID experiments. Signal detection was performed with a reflector, microchannel plate (MCP) detector and time-to-digital converter. Mass calibration was carried out using a NaI/CsI standard solution from *m*/*z* 50–1000. Data acquisition and processing were carried out using software MassLynx NT version 3.5 supplied with the instrument. The MS survey range was *m*/*z* 50–1000, with a scan duration of 1.0 s and an interscan delay of 0.1 s. Each mass spectrum was recorded over a period of one second and mass spectra were accumulated over a period of at least 60 s for both single analyzer profiles and CID experiments. For each of the ion species examined, the lock mass in each product ion mass spectrum was the calculated monoisotopic mass/charge ratio of the precursor ion.

## 3. Results and discussion

### 3.1. Nomenclature

The nomenclature system for flavonoid aglycones, as developed by Mabry and Markham [46] for the definition of the various A and B ring fragments generated by EI, was found to be inadequate for describing the range of product ions formed when protonated molecules are subjected to CID [47,48]. A more systematic ion nomenclature for flavonoid aglycones has been proposed [49] that is conceptually similar to that introduced for the description of carbohydrate fragmentations in product ion mass spectra of glycoconjugates [50]. The numbering scheme for substitution in isoflavones is shown in Scheme 1. The nomenclature and diagnostic fragmentations of genistein-7-*O*-glucoside are shown in Scheme 2. For free aglycones, the $^{i,j}A^+$ (or $^{i,j}A^-$) and the $^{i,j}B^+$ labels designate primary product ions containing intact A and B rings, respectively, in which the superscripts indicate the C-ring bonds that have been broken. In Scheme 2, the C-ring bonds and the glucose ring bonds are numbered with a small font, the carbon atoms in the A, B, and C rings are labeled with a larger font, and the primary fragmentations are indicated. Ions resulting from cross-ring cleavages in the sugar residue are denoted with X labels.

### 3.2. Deprotonated genistein-7-O-glucoside

The product ion mass spectrum for deprotonated genistein-7-*O*-glucoside, *m*/*z* 431, obtained at a collision energy of 47 eV is shown in Fig. 1. Initially, the collision energy was maintained at 4 eV so as to transmit precursor ions of *m*/*z* 431 in order to obtain a well-shaped peak for this ion species; then, after 1 min, the collision energy was increased to 47 eV for 3 min in order to observe the fragment ions of *m*/*z* 431. The parent ion peak (*m*/*z* 431.0978) was used as a lock mass for the product ion mass spectrum of Fig. 1. The structure of deprotonated genistein-7-*O*-glucoside is given in Scheme 2 together with the possible diagnostic fragmentations of the glucose and genistein moieties and loss of the glycan residue.

The product ion mass spectrum for deprotonated genistein-7-*O*-glucoside (Fig. 1) obtained with an ES source is rather simple and the relatively few fragmentations observed are depicted in Scheme 3. *m*/*z* 269 is the $Y_o^-$ ion showing the loss of a $C_6H_{10}O_5$ (162 Da) moiety; here, the

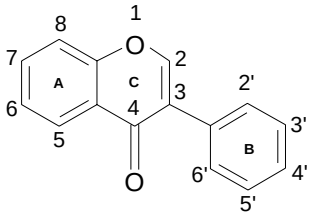


Scheme 1. Isoflavone numbering scheme.

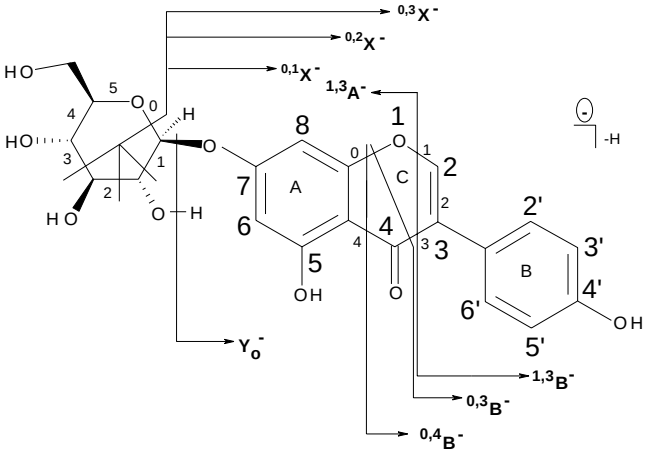


Scheme 2. Nomenclature and diagnostic fragmentations of genistein-7-*O*-glucoside.

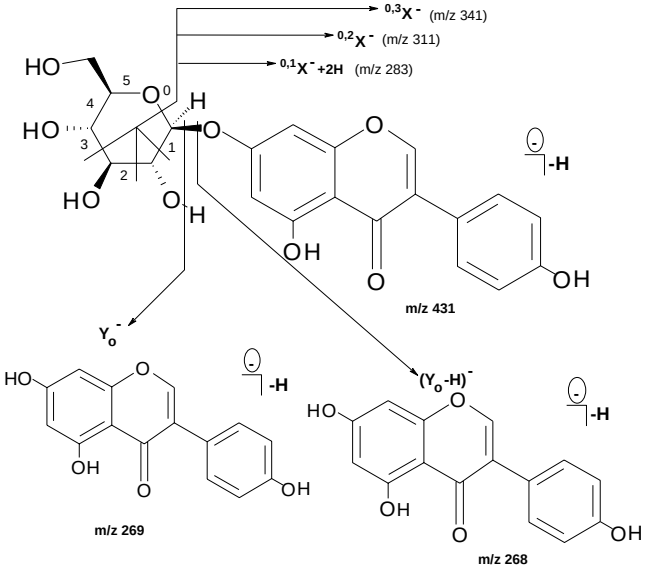


Scheme 3. Primary fragmentations of deprotonated genistein-7-*O*-glucoside.

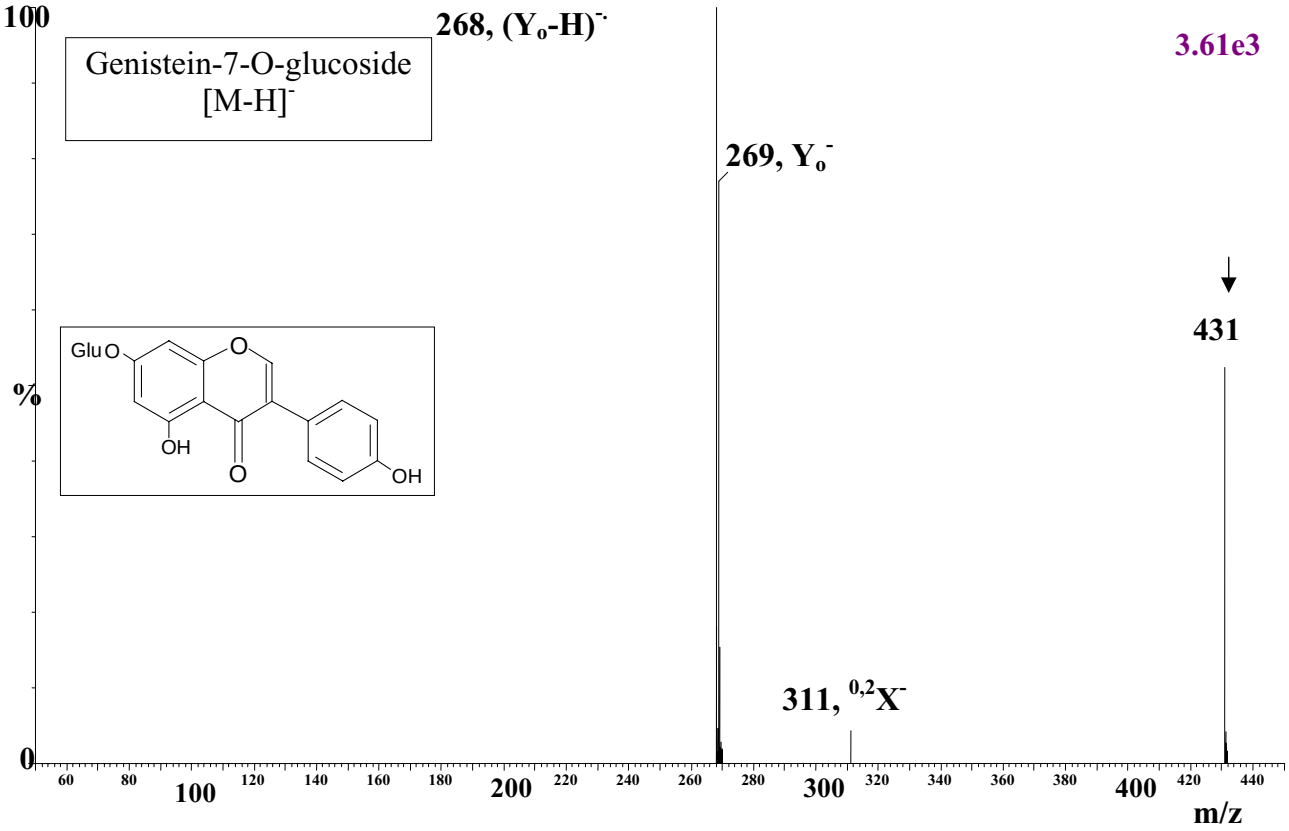


Fig. 1. Product ion mass spectrum of deprotonated genistein-7-*O*-glucoside, *m*/*z* 431.0978, obtained at a collision energy of 47 eV.

hydrogen atom of the hydroxyl group attached to the sugar C atom vicinal to that involved in the glycosidic linkage is transferred to the fragment ion in a rearrangement reaction. For flavonoid *O*-glycosides it has been demonstrated using deuterium labeling that a hydroxyl hydrogen atom participates in this rearrangement reaction and remains with the $Y_o^-$ ion [51]. The corresponding pure scission process yields a $(Y_o - H)^{\bullet -}$ ion of *m*/*z* 268 that forms the base peak in this product ion mass spectrum at a collision energy of 47 eV. In general, the energy of activation for a rearrangement reaction is less than that for a scission process such that, at low collision energies (~15–30 eV), the rearrangement reaction product dominates. However, as collision energy is increased, the ion signal intensity of the scission product increases relative to that of the rearrangement product; such is the case here. The variation of the ratio of ion signal intensities of *m*/*z* 268 $(Y_o - H)^{\bullet -}$ and *m*/*z* 269 ($Y_o^-$) is shown in Fig. 2. In this figure, the collision energy is expressed in the center-of-mass ($E_{cm}$) frame where $E_{cm} = E_{lab}$ (target mass/sum of target mass and projectile mass); $E_{lab}$ is the collision energy in the laboratory frame. For example, when *m*/*z* 431 impinges upon argon target gas with a collision energy in the laboratory frame of 45 eV, the value of $E_{cm}$ is 3.8 eV. At an $E_{cm}$ of 3.8 eV, the ratio of ion signal intensities of *m*/*z* 268 $(Y_o - H)^{\bullet -}$ and *m*/*z* 269 ($Y_o^-$) as shown in Fig. 2 is close to unity. When the collision energy is increased further, fragmentation of the $(Y_o - H)^{\bullet -}$ and $Y_o^-$ ions is observed.

Hvattum [52] reported the observation from $[M - H]^-$ (*m*/*z* 447) of quercitrin (5,7,3′,4′-tetrahydroxyflavone-3-*O*-rhamnose) of the aglycone fragment ($Y_o^-$) at *m*/*z* 301 and the radical aglycone anion $(Y_o - H)^{\bullet -}$ at *m*/*z* 300. Subsequently, Hvattum and Ekeberg [53] reported a systematic study of the ability of flavonoid glycosides to generate both negative ion collision-induced heterolytic and homolytic cleavage. They found that the relative abundance of the radical aglycone to the aglycone product ion increased with increasing collision energy and with increasing number of

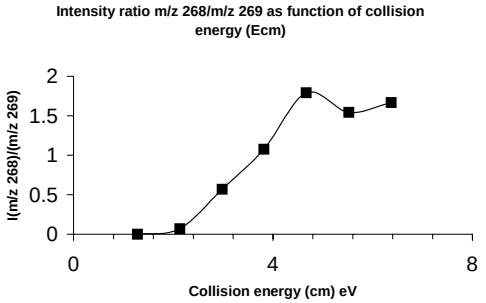


Fig. 2. Variation of the ion signal intensity ratio of $(Y_o - H)^{\bullet -}$ (*m*/*z* 268):$Y_o^-$ (*m*/*z* 269) with the collision energy in the center-of-mass frame.

hydroxyl substituents in the B ring. Furthermore, they observed that the nature and position of the sugar substitution of the flavonoid glycosides also affected fragmentation to the radical aglycone. The findings of recent studies [54,55] are in agreement with the observations of Hvattum and Ekeberg with respect to radical aglycone formation from $[M-H]^-$ of apigenin-7-*O*-glucoside and luteolin-7-*O*-glucoside; in these same studies, radical aglycone formation from $[M-H]^-$ of kaempferol-7-*O*-glucoside and quercitin-3-*O*-rutinoside was reported together with radical aglycone formation from $[M+H]^+$ of luteolin-8-*C*-glucoside. Radical aglycone formation was not observed from $[M-H]^-$ of luteolin-4′-*O*-glucoside. Radical aglycone formation is of interest because the ability of a flavonoid glycoside to provide a radical aglycone is possibly related to the electron- or hydrogen-donating antioxidant activity of the flavonoid. The product ion mass spectra of the $(Y_o-H)^{\bullet-}$ and $Y_o^-$ ions from $[M-H]^-$ of genistein-7-*O*-glucoside are discussed below.

In addition to the $(Y_o-H)^{\bullet-}$ and $Y_o^-$ fragment ions, three $X^-$-type fragment ions were observed as a result of bond cleavages in the glucose moiety as shown in Scheme 3. The ion signal intensity of the $^{0,2}X^-$ species (*m/z* 311) was ~6% of that of the base peak and those of the $^{0,1}X^- + 2H$ (*m/z* 283) and $^{0,3}X^-$ (*m/z* 341) fragment ions were ~1% of that of the base peak. Formation of each of the $^{0,1}X^- + 2H$, $^{0,2}X^-$, and $^{0,3}X^-$ species is accompanied by the loss of $C_5H_8O_5$, $C_4H_8O_4$, and $C_3H_6O_3$, respectively. Observation of the $^{0,1}X^- + 2H$ ion indicates that two hydrogen atoms have transferred to the carbon atom bonded to the oxygen atom at the 7 position, possibly to form deprotonated genistein-7-*O*-methoxy. No fragmentation of the genistein moiety was observed.

### 3.2.1. Product ion mass spectra of $(Y_o-H)^{\bullet-}$ and $Y_o^-$ ions

The $(Y_o-H)^{\bullet-}$ and $Y_o^-$ ion species were examined further because fragmentation of these species may be indicative of the location of the glycoside moiety in genistein glycosides. The product ion mass spectra of the $(Y_o-H)^{\bullet-}$ and $Y_o^-$ ion species are shown in Figs. 3 and 4, respectively. In each case, the $(Y_o-H)^{\bullet-}$ or $Y_o^-$ ion species was transmitted by the quadrupole mass filter and passed into the collision cell at an $E_{lab}$ of 4 eV and the ion signal intensity of the $(Y_o-H)^{\bullet-}$ or $Y_o^-$ ion species was monitored. An $E_{lab}$ of 4 eV is insufficient in most cases to bring about dissociation of the isolated ion species. The cone voltage was varied from 10 to 100 V while the ion signal intensity was monitored.

The product ion mass spectra shown in Figs. 3 and 4 differ substantially from each other, particularly with respect to the number of fragments ion species observed in each mass spectrum, therefore the fragmentation pathways of the $(Y_o-H)^{\bullet-}$ and $Y_o^-$ ions differ. The observed loss of a hydrogen atom from the $Y_o^-$ ion could have produced a $[Y_o^- - H^\bullet]$ ion that would exhibit the same fragmentations as the $(Y_o-H)^{\bullet-}$ ion; such was not the case. The product ion mass spectra shown in Figs. 3 and 4 were investigated further by accurate mass measurement and by determination of the product ion–precursor ion relationship for each of the principal fragment ions observed in the product ion mass spectra shown in Figs. 3 and 4.

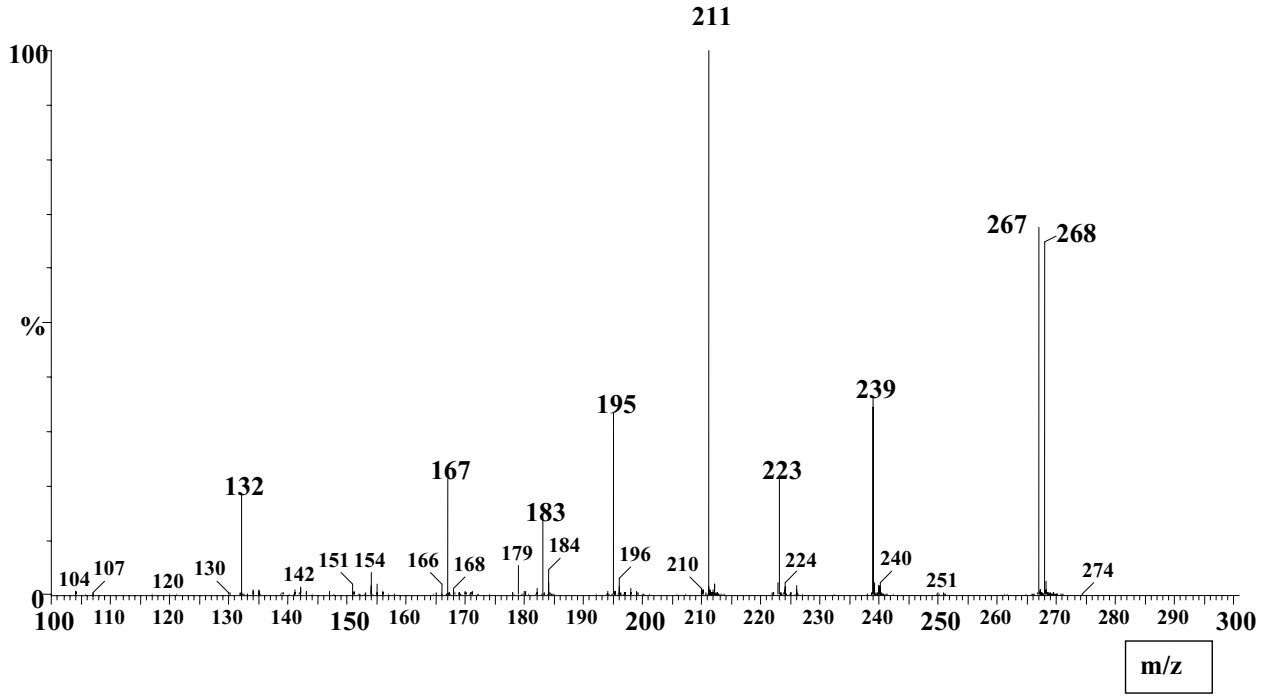


Fig. 3. Product ion mass spectrum of the $(Y_o-H)^{\bullet-}$ ion (*m/z* 268) from genistein-7-*O*-glucoside.

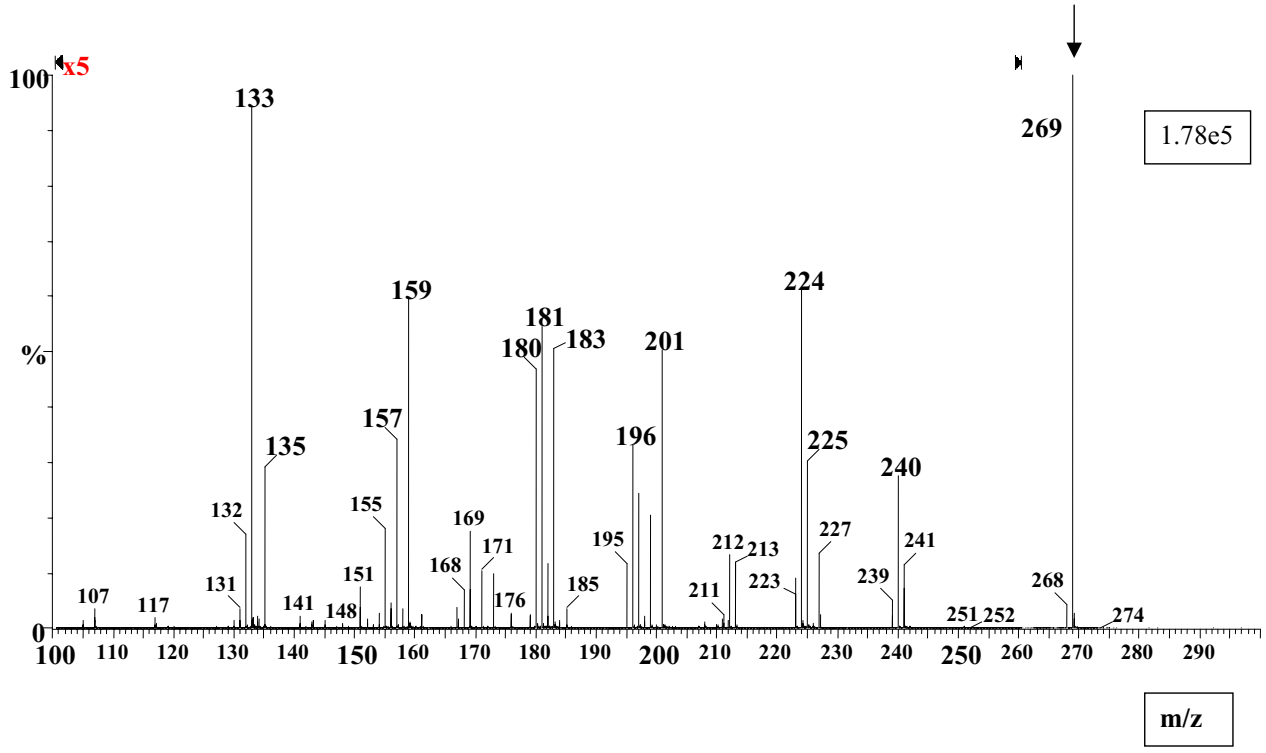


Fig. 4. Product ion mass spectrum of the $Y_o^-$ ion (*m*/*z* 269) from genistein-7-*O*-glucoside.

### 3.2.2. Accurate mass measurement

In the product ion mass spectrum of the $(Y_o - H)^{\bullet -}$ ion (Fig. 3), there are nine principal fragment ion species. The empirical formula, observed and calculated mass/charge ratios, double bond equivalents, and mass errors are given in Table 1. The errors between the observed masses and calculated ones ranged from 0 to −3.9 mDa (0–30 ppm) with an average value of −1.4 mDa (−9.5 ppm) indicating good mass accuracy. It should be noted that a mass defect of 1.0 mDa for an ion of low mass/charge ratio, say *m*/*z* 200, yields an error of 5 ppm which is not inordinately high for small mass/charge ratio ions. Furthermore, for an ion of *m*/*z* 200, there are few different elemental compositions that satisfy the requirements of the elemental composition of the known parent ion therefore the elemental composition of a fragment ion can be obtained with a high degree of confidence. In Fig. 4, there are some 30 principal fragment ion species and the empirical formula, observed and calculated mass/charge ratios, double bond equivalents, and mass errors of these fragment ions are given in Table 2. The errors between the observed masses and calculated ones ranged from 0.3 to −6.0 mDa (1.4–45 ppm) with an average value of −2.3 mDa (−14 ppm).

### 3.2.3. Fragmentation schemes

As may be expected, there are some fragment ions that are common to the fragmentations observed for each of the $Y_o^-$ and $(Y_o - H)^{\bullet -}$ ions; these fragment ions are of *m*/*z* 239,

Table 1
Empirical formula, observed and calculated mass/charge ratios, double bond equivalents (DBE), and mass errors of the principal fragment ions observed in the product ion mass spectrum of $(Y_o - H)^{\bullet -}$ (*m*/*z* 268)

| Predicted formula | Observed mass (Da) | Calculated mass (Da) | DBE | Error (mDa) | Error (ppm) |
|---|---|---|---|---|---|
| $C_{15}H_8O_5^-$ | 268.0372 | 268.0372 | 12.0 | – | – |
| $C_{15}H_7O_5^-$ | 267.0282 | 267.0293 | 12.5 | −1.1 | −4.3 |
| $C_{14}H_7O_4^-$ | 239.0344 | 239.0344 | 11.5 | 0.0 | −0.1 |
| $C_{14}H_7O_3^-$ | 223.0380 | 223.0395 | 11.5 | −1.5 | −6.8 |
| $C_{13}H_7O_3^-$ | 211.0379 | 211.0395 | 10.5 | −1.6 | −7.7 |
| $C_{13}H_7O_2^-$ | 195.0446 | 195.0446 | 10.5 | 0.0 | 0.0 |
| $C_{12}H_7O_2^-$ | 183.0431 | 183.0446 | 9.5 | −1.5 | −8.2 |
| $C_{12}H_7O^-$ | 167.0472 | 167.0497 | 9.5 | −2.5 | −15.0 |
| $C_{11}H_6O^-$ | 154.0410 | 154.0419 | 9.0 | −0.9 | −5.6 |
| $C_8H_4O_2^-$ | 132.0172 | 132.0211 | 7.0 | −3.9 | −30.0 |
| Average | | | | −1.4 | −9.5 |

Table 2
Empirical formula, observed and calculated mass/charge ratios, double bond equivalents (DBE), and mass errors of the principal fragment ions observed in the product ion mass spectrum of $Y_o^-$ (*m*/*z* 269)

| Predicted formula | Observed mass (Da) | Calculated mass (Da) | DBE | Error (mDa) | Error (ppm) |
|---|---|---|---|---|---|
| $C_{15}H_9O_5^-$ | 269.0450 | 269.0450 | 11.5 | – | – |
| $C_{14}H_9O_4^-$ | 241.0487 | 241.0501 | 10.5 | −1.4 | −5.7 |
| $C_{14}H_8O_4^-$ | 240.0404 | 240.0423 | 11.0 | −1.9 | −7.7 |
| $C_{14}H_7O_4^-$ | 239.0367 | 239.0344 | 11.5 | 2.3 | 9.5 |
| $C_{13}H_7O_4^-$ | 227.0354 | 227.0344 | 10.5 | 1.0 | 4.3 |
| $C_{14}H_9O_3^-$ | 225.0538 | 225.0552 | 10.5 | −1.4 | −6.1 |
| $C_{14}H_8O_3^-$ | 224.0477 | 224.0473 | 11.0 | 0.4 | 1.6 |
| $C_{14}H_7O_3^-$ | 223.0403 | 223.0395 | 11.5 | 0.8 | 3.5 |
| $C_{13}H_9O_3^-$ | 213.0559 | 213.0552 | 9.5 | 0.7 | 3.4 |
| $C_{13}H_8O_3^-$ | 212.0457 | 212.0473 | 10.0 | −1.6 | −7.8 |
| $C_{13}H_7O_3^-$ | 211.0345 | 211.0395 | 10.5 | −5.0 | −24.0 |
| $C_{12}H_9O_3^-$ | 201.0546 | 201.0552 | 8.5 | −0.6 | −2.8 |
| $C_{12}H_7O_3^-$ | 199.0398 | 199.0395 | 9.5 | 0.3 | 1.4 |
| $C_{13}H_9O_2^-$ | 197.0615 | 197.0603 | 9.5 | 1.2 | 6.3 |
| $C_{13}H_8O_2^-$ | 196.0507 | 196.0524 | 10.0 | −1.7 | −8.8 |
| $C_{13}H_7O_2^-$ | 195.0457 | 195.0446 | 10.5 | 1.1 | 5.6 |
| $C_{12}H_7O_2^-$ | 183.0441 | 183.0446 | 9.5 | −0.5 | −2.8 |
| $C_{12}H_6O_2^-$ | 182.0348 | 182.0368 | 10.0 | −2.0 | −11.0 |
| $C_{13}H_9O^-$ | 181.0637 | 181.0653 | 9.5 | −1.6 | −9.1 |
| $C_{13}H_8O^-$ | 180.0564 | 180.0575 | 10.0 | −1.1 | −6.2 |
| $C_{11}H_9O_2^-$ | 173.0553 | 173.0603 | 7.5 | −5.0 | −29.0 |
| $C_{11}H_7O_2^-$ | 171.0414 | 171.0446 | 8.5 | −3.2 | −19.0 |
| $C_{12}H_9O^-$ | 169.0640 | 169.0653 | 8.5 | −1.3 | −7.9 |
| $C_{12}H_8O^-$ | 168.0545 | 168.0575 | 9.0 | −3.0 | −18.0 |
| $C_{12}H_7O^-$ | 167.0467 | 167.0497 | 9.5 | −3.0 | −18.0 |
| $C_{10}H_7O_2^-$ | 159.0414 | 159.0446 | 7.5 | −3.2 | −20.0 |
| $C_{10}H_5O_2^-$ | 157.0347 | 157.0290 | 8.5 | 5.7 | 37.0 |
| $C_{11}H_7O_2^-$ | 155.0448 | 155.0497 | 8.5 | −4.9 | −32.0 |
| $C_4H_7O_5^-$ | 135.0267 | 135.0293 | 1.5 | −2.6 | −19.0 |
| $C_8H_5O_2^-$ | 133.0230 | 133.0290 | 6.5 | −6.0 | −45.0 |
| $C_8H_4O_2^-$ | 132.0155 | 132.0211 | 7.0 | −5.6 | −42.0 |
| Average | | | | −2.3 | −14.0 |

223, 211, 195, 183, 167, and 132. However, for only one common fragment ion, *m*/*z* 183, is the ion signal intensity relative to that of the base peak greater for the $Y_o^-$ ion. Thus the dominant fragmentation patterns for each of the $Y_o^-$ and $(Y_o - H)^{\bullet -}$ ions differ but the overall fragmentation pattern for the $Y_o^-$ ion includes a few of the features of that of the $(Y_o - H)^{\bullet -}$ ion.

In Scheme 4 is shown the fragmentation scheme for the $(Y_o - H)^{\bullet -}$ ion of *m*/*z* 268. The fragment ion structures proposed in this scheme are plausible on the basis of chemical intuition but are not definitive. Each arrow in Scheme 4 represents an experimentally-determined direct product ion–precursor ion relationship; that is, each precursor ion was isolated and subjected to CID as the collision energy was increased whereupon the product ion shown near the head of each arrow was observed as a direct fragment ion of the precursor. The mass/charge ratio of both the precursor and product ions were measured to within about 1 mDa and the corresponding elemental compositions were determined. In this manner, each fragmentation step of the $(Y_o - H)^{\bullet -}$ ion of *m*/*z* 268 was determined. Two structures for *m*/*z* 268, I and II, are shown in Scheme 4 for *m*/*z* 268: structure I is the radical anion where, presumably, one of the two hydroxy hydrogen atoms has been lost, and the A, B, and C rings remain intact; structure II has a modified C ring and has been invoked here because of the need to explain the loss of $CO_2$ from *m*/*z* 267. Elimination of $CO_2$ from an ion requires that the two oxygen atoms be separated by not more than two carbon atoms and this condition is not satisfied by structure I; thus, structure II has been invoked.

The sole primary fragmentation product of C-ring cleavage is the $[^{0,3}B - H]^{\bullet -}$ ion of *m*/*z* 132. In the stepwise fragmentation of flavonoids, the basic $C_{15}$ skeleton suffers losses of carbon atoms yet the A and B rings remain initially intact within the fragment ions and, eventually, become bonded together in a fused tricyclic structure prior to major fragmentation of the A and B rings. Initial losses of carbon atoms occur from the C ring by C-ring opening, rotation of the B ring about its bond with the C ring and bonding of the B ring to the A ring at the B-ring 2′ site. Formation of structure II may occur by scission of the bond between $C_4$ and the A ring followed by a reduction in the bond order of the $C_2$–$C_3$ bond, rotation about the $C_2$–$C_3$ bond, and bond formation between the $C_{2'}$ and the A ring to form a seven-membered

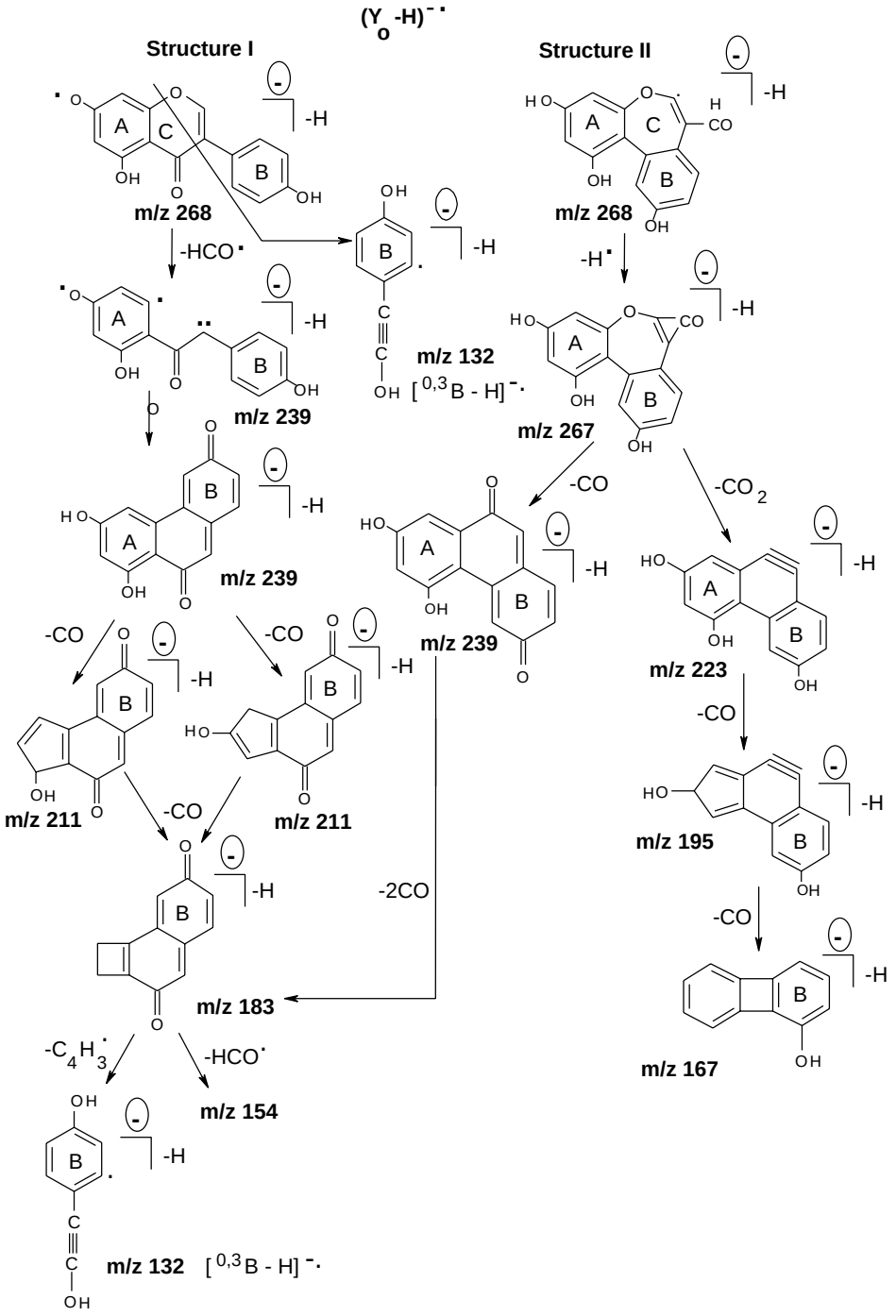


Scheme 4. Fragmentation scheme for the $(Y_o - H)^{\bullet -}$ ion (*m*/*z* 268).

C ring. The $C_4$ keto group is no longer bonded within the C ring but is attached to it. Hydrogen atom migration from the $C_2$ carbon to the keto group attached to the C ring completes the formation of structure II. Upon loss of a hydrogen atom from the aldehyde group to form *m*/*z* 267, the CO moiety becomes bonded to both $C_2$ and $C_3$. The structure for *m*/*z* 267 now presents two oxygen atoms separated by but two carbon atoms and the subsequent loss of $CO_2$ to form *m*/*z* 223 is facile. Further losses of CO from *m*/*z* 223 to form *m*/*z* 195 and 167 involve the loss of hydroxyl oxygen atoms and skeleton carbon atoms leading to ring shrinkage and the formation of highly unsaturated ions. Although the structures proposed for *m*/*z* 195 and 167 are highly speculative, these structures provide useful reference points for an ongoing computational study of ions derived from flavonoids and flavonoid glycosides.

The loss of HCO• from the radical negatively-charged structure I for *m*/*z* 268 to form *m*/*z* 239 involves the loss of the $C_2$ carbon and the ring oxygen. The expulsion of HCO• that is shown to lead to an intermediate having four unpaired electrons initially is accompanied by B ring rotation about the $C_3$–$C_4$ bond, and bond formation between the $C_{2'}$ and the A ring to form a six-membered C ring. It should be noted that the *m*/*z* 239 ions from structures I and II are isomers and they differ in their behavior. The further fragmentation of both species of *m*/*z* 239 is constrained by the necessity to explain the subsequent formation of *m*/*z* 132 that is identified as the $[^{0,3}B - H]^{\bullet -}$ species observed also as a primary fragmentation product of structure I. Thus, the *m*/*z* 239 species from structure I loses CO from the A ring to form *m*/*z* 211; as there are two possible sites on the A ring for loss of CO, two isomeric forms of *m*/*z* 211 are proposed. The subsequent loss of a second CO molecule from each of the two forms of *m*/*z* 211 leads to the proposed structure for *m*/*z* 183; this structure is common not only for CO loss from the two forms of *m*/*z* 211 but for the loss of 2CO from *m*/*z* 239 obtained from structure II. The *m*/*z* 183 species formed indirectly from each of structures I and II loses both $C_4H_3$• and HCO•. The loss of $C_4H_3$• leads directly to the formation of *m*/*z* 132 for which the proposed structure is identical to that of the $[^{0,3}B - H]^{\bullet -}$ species formed as a primary fragmentation product of structure I.

In Scheme 5 is shown the fragmentation scheme for the $Y_o^-$ ion of *m*/*z* 269. Each arrow in Scheme 5 represents an experimentally-determined direct product ion–precursor ion relationship. The principal primary fragmentation product of C-ring cleavage is the $^{0,3}B^-$ ion of *m*/*z* 133 for which the structure has been proposed [38] as HO–C≡C–($C_6H_4$)–$O^-$; *m*/*z* 133 is the base peak in the product ion mass spectrum and is a diagnostic ion for deprotonated genistein. Support for the proposed structure of *m*/*z* 133 is forthcoming from the product ion mass spectrum of $[M - H]^-$ from daidzein (7,4′-dihydroxy isoflavone); the B and C rings of daidzein are identical with those for genistein, and *m*/*z* 133 is observed as a major fragment ion in this product ion mass spectrum also. Other primary fragmentation products of C-ring cleavage observed are the $^{1,3}B^-$ (*m*/*z* 117, 2%), $^{0,4}B^-$ (*m*/*z* 161, 2%), and $^{1,3}A^-$ (*m*/*z* 151, 8%) ion species where the percentage refers to the ion signal intensity relative to the $^{0,3}B^-$ ion of *m*/*z* 133. The loss of $CO_2$ from *m*/*z* 269 presents the same problem as above but with respect to the structure of *m*/*z* 269. It is probable that two structures for *m*/*z* 269 must be invoked to explain the subsequent fragmentations and that these structures will be similar to structures

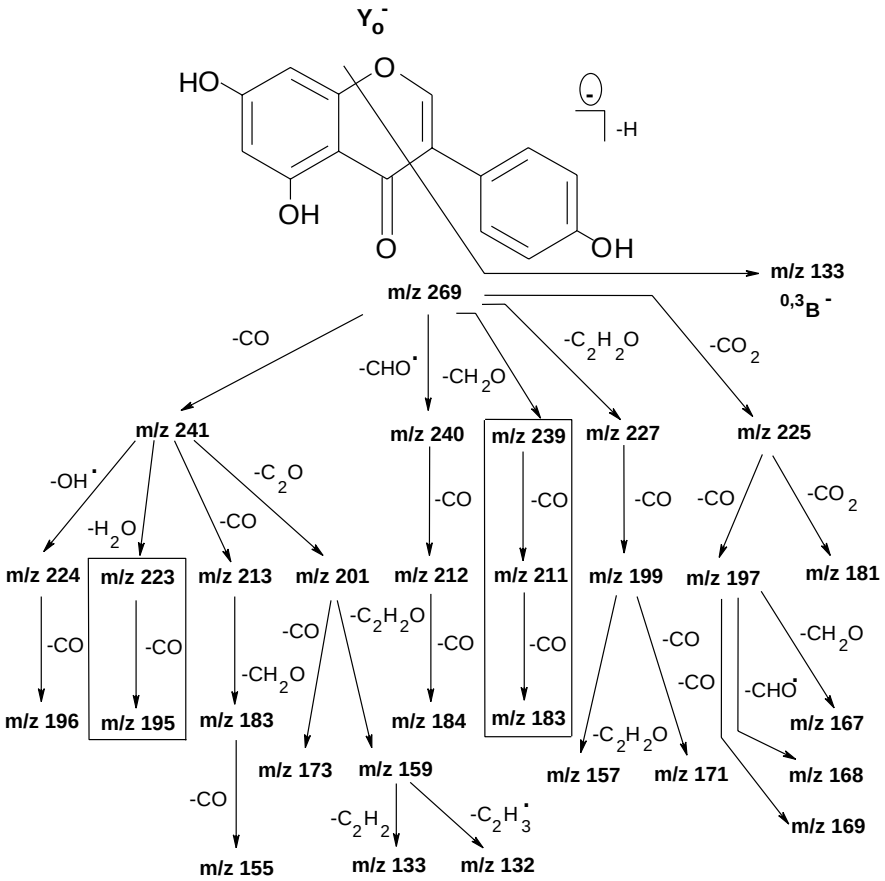


Scheme 5. Fragmentation scheme for the $Y_o^-$ ion (*m*/*z* 269). Parts of the fragmentation scheme for *m*/*z* 269 shown here in boxes are identical to the corresponding parts of the fragmentation scheme for *m*/*z* 268 shown in Scheme 4.

I and II for *m*/*z* 268. Two parts of the fragmentation scheme for *m*/*z* 269 shown in boxes in Scheme 5 are identical to the corresponding parts of the fragmentation scheme for *m*/*z* 268 shown in Scheme 4. The multiple losses of CO shown in Scheme 5 are primarily due to the thermodynamic stability of this molecule relative to those of the CO-containing small molecules $CH_2O$ and $C_2H_2O$ and the $CHO^{\bullet}$ radical.

Fabre et al. [41] have described in tabular form a product ion mass spectrum of $[M - H]^-$ (*m*/*z* 269) of the aglycone genistein obtained with ES and an ion trap mass spectrometer. All of the reported ion species (*m*/*z* 241, 227, 225, 201, 197, 183, 181, and 159) were observed also in the product ion mass spectrum shown in Fig. 4, along with many other ion species. No fragmentation products of C-ring cleavage were reported. Fabre et al. [41] proposed a fragmentation scheme incorporating ion structures for $[M - H]^-$ from luteolin and, by analogy, for the eight fragment ions given above from $[M - H]^-$of genistein. No alternative scheme is proposed here. However, part of the proposed fragmentation scheme involved the loss of $C_3O_2$ from *m*/*z* 269 to form *m*/*z* 201; this fragmentation was not observed in the work reported here, rather successive losses of CO and $C_2O$ from *m*/*z* 269 and *m*/*z* 241, respectively, were observed.

### 3.3. Protonated genistein-7-O-glucoside

The product ion mass spectrum of protonated genistein-7-*O*-glucoside $[M + H]^+$ of *m*/*z* 433 is shown in Fig. 5. The principal neutral moiety lost is the glycan residue of $C_6H_{10}O_5$ (162 Da) to form the $Y_o^+$ ion of *m*/*z* 271. The fragment ions of *m*/*z* <271 shown in Fig. 5 with 20× magnification were observed at an optimum collision energy of 34 eV and those of *m*/*z* >271 and <433, also with 20× magnification, were observed at an optimum collision energy of 17 eV. The ion signal intensities of the fragment ions of *m*/*z* >271 and <433 were generally much weaker (∼10%) of those of fragment ions of *m*/*z* <271. The fragment ions of *m*/*z* >271 and <433 arose from fragmentation of the glucose moiety and these fragmentations were much more extensive than those observed at a similar collision energy for the negatively-charged deprotonated molecule.

While the ion signal intensities of the fragment ions of *m*/*z* >271 and <433 were too low to permit accurate mass determination and observation of product ion mass spectra of the individual fragment ions, several ion species may be identified tentatively. The principal fragmentations of the glucose moiety are shown in Scheme 6. *m*/*z* 401 can be formed by the loss of the primary alcohol group as methanol and *m*/*z* 387 by 4, 5 scission with the loss of the elements of ethanol.

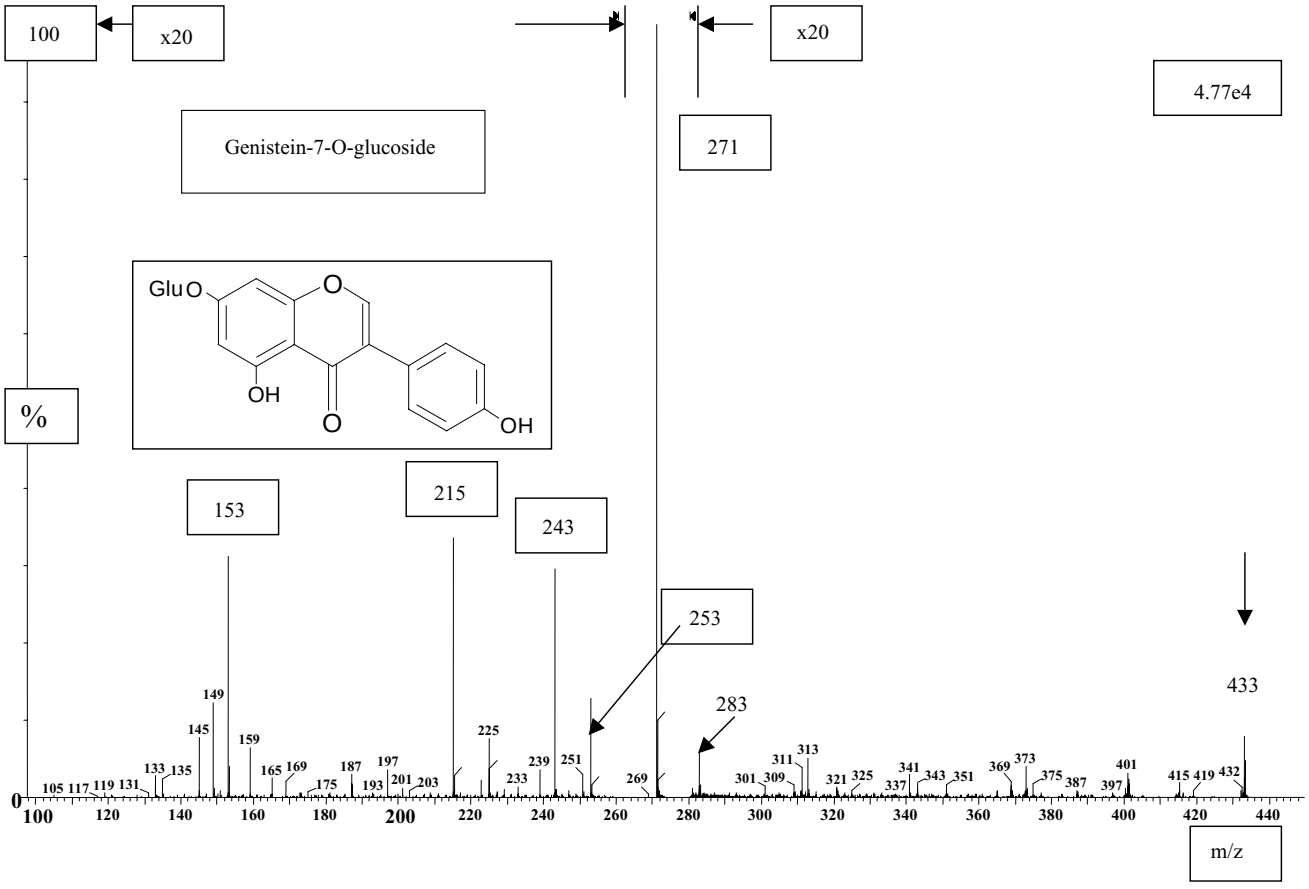


Fig. 5. Product ion mass spectrum of protonated genistein-7-*O*-glucoside $[M + H]^+$ of *m*/*z* 433.

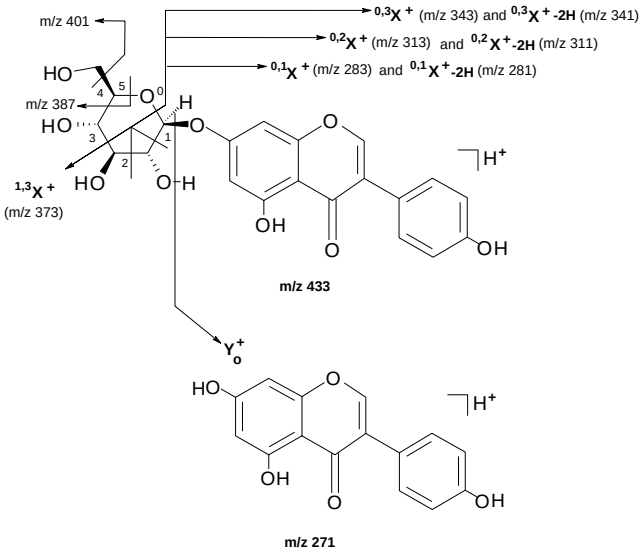


Scheme 6. Primary fragmentations of protonated genistein-7-*O*-glucoside (*m*/*z* 433).

Further fragmentations of the glucose moiety gave rise to the $^{1,3}X^+$, $^{0,3}X^+$, $^{0,3}X^+ - 2H$, $^{0,2}X^+$, $^{0,2}X^+ - 2H$, $^{0,1}X^+$, and $^{0,1}X^+ - 2H$ ions at *m*/*z* 373, 343, 341, 313, 311, 283, and 281, respectively. The ions of *m*/*z* 415, 397, and 369 (not shown in Scheme 6) are associated with the loss of 1–3 water molecules, respectively. The extensive fragmentation of the glucose moiety in protonated genistein-7-*O*-glucoside, though of low ion signal intensity, contrasts sharply with the investigation in this laboratory of the product ion mass spectrum of protonated luteolin-4′-*O*-glucoside in which no fragmentations of the glucose moiety were observed and that of protonated apigenin-8-*C*-glucoside for which glucose moiety fragmentation was both extensive and of relatively high ion signal intensity.

The ion signal intensities of the fragment ions of *m*/*z* <271 are in good agreement with the product ion mass spectrum of protonated genistein. The empirical formula, observed and calculated mass/charge ratios, double bond equivalents, and mass errors of the fragment ions of *m*/*z* <271 are given in Table 3. The errors between the observed masses and calculated ones ranged from 0 to 1.1 mDa (0–5.3 ppm) with an average value of 0.7 mDa (2.9 ppm). The ion signal intensity of *m*/*z* 187 was so low that the peak shape was far from ideal and produced a relatively large error in the peak centroid. The pattern of principal fragmentations of $Y_o^+$ ions of *m*/*z* 271 is shown in Scheme 7.

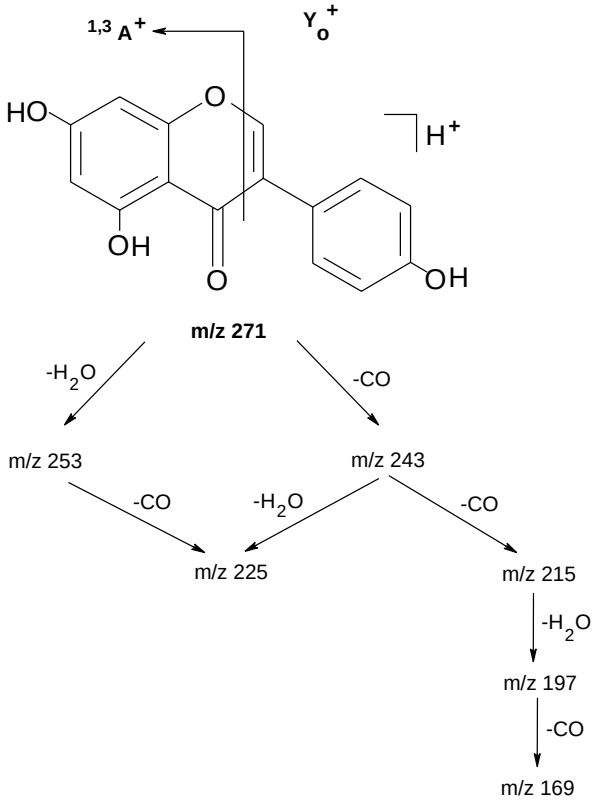


Scheme 7. Fragmentation of the $Y_o^+$ ion (*m*/*z* 271) from protonated genistein-7-*O*-glucoside.

## 4. Conclusion

Low-energy product ion mass spectra of the $[M + H]^+$ and $[M - H]^-$ ions of genistein-7-*O*-β-D-glucoside (5,7,4′-

Table 3
Empirical formula, observed and calculated mass/charge ratios, double bond equivalents (DBE), and mass errors of the principal fragment ions observed in the product ion mass spectrum of $Y_o^+$ (*m*/*z* 271)

| Predicted formula | Observed mass (Da) | Calculated mass (Da) | DBE | Error (mDa) | Error (ppm) |
|---|---|---|---|---|---|
| $C_{15}H_{11}O_5^+$ | 271.0606 | 271.0606 | 10.5 | – | – |
| $C_{15}H_9O_4^+$ | 253.0506 | 253.0501 | 11.5 | 0.5 | 2.0 |
| $C_{14}H_{11}O_4^+$ | 243.0663 | 243.0657 | 9.5 | 0.6 | 2.3 |
| $C_{14}H_9O_3^+$ | 225.0559 | 225.0552 | 10.5 | 0.7 | 3.2 |
| $C_{13}H_{11}O_3^+$ | 215.0719 | 215.0708 | 8.5 | 1.1 | 5.0 |
| $C_{13}H_9O_2^+$ | 197.0613 | 197.0603 | 9.5 | 1.0 | 5.3 |
| $C_{12}H_{11}O_2^+$ | 187.0759 | 187.0759 | 7.5 | 0.0 | 0.0 |
| $C_{12}H_9O^+$ | 169.0650 | 169.0653 | 8.5 | −0.3 | 2.0 |
| $C_7H_5O_4^+$ | 153.0183 | 153.0188 | 5.5 | −0.5 | 3.2 |
| Average | | | | −0.7 | 2.9 |

trihydroxyisoflavone) show simple fragmentation patterns that permit characterization of the substituents in the A and B rings. $[M - H]^-$ ions show neutral losses of 162 and 163 Da by rearrangement and scission, respectively, leading to aglycone and radical aglycone product ion formation; radical aglycone formation dominates at higher collision energies. $[M + H]^+$ ions also show a neutral loss of 162 Da but the scission reactions whereby losses of 161 or 163 Da would be expected were not observed. Fragmentation of the glucose moiety in $[M + H]^+$ ions, though of low ion signal intensity, was more extensive than that observed from $[M - H]^-$ ions. Fragmentation mechanisms and structures of fragment ions from $(Y_o - H)^{\bullet -}$ (*m*/*z* 268) have been proposed. Observation of product ion mass spectra of mass-selected primary and secondary fragment ions formed in the source was facilitated by the use of elevated cone voltages. The examination of product ion mass spectra at high mass resolution allowed unambiguous determination of the elemental composition of fragment ions. Characterization of the fragmentation patterns for $[M + H]^+$ and $[M - H]^-$ ions of genistein-7-*O*-β-D-glucoside is facilitating a current investigation of flavonoid glycosides in this laboratory.

## Acknowledgements

The authors acknowledge the financial support from each of the Natural Sciences and Engineering Research Council of Canada (Discovery Grants Program), the Canada Foundation for Innovation, the Ontario Research & Development Challenge Fund and Trent University. The authors acknowledge with grateful thanks the guidance and counsel of a reviewer.

## References

[1] J.B. Harborne (Ed.), The Flavonoids: Advances in Research since 1986, Chapman and Hall, London, 1994.
[2] E. Sjostrom, Wood Chemistry Fundamentals and Applications, Academic Press Inc., New York, London, 1981.
[3] E.C. Bate-Smith, in: W.E. Hillis (Ed.), Wood Extractives and their Significance to the Pulp and Paper Industries, Academic Press Inc., New York, London, 1962, p. 133.
[4] J.B. Harborne, R.J. Grayer, in: J.B. Harborne (Ed.), The Flavonoids: Advances in Research since 1986, Chapman and Hall, London, 1994, p. 589.
[5] V. Beck, E. Unterrieder, L. Krenn, W. Kubelka, A. Jungbauer, J. Ster. Biochem. Mol. Biol. 84 (2003) 259.
[6] S.M. Boue, T.E. Wiese, S. Nehls, M.E. Burow, S. Elliott, C.H. Carter-Wientjes, B.Y. Shih, J.A. McLachlan, T.E. Cleveland, J. Agric. Food Chem. 51 (2003) 2193.
[7] B.W. Shirley, Trends Plant Sci. 1 (1996) 377.
[8] K.L. Fritz, C.M. Seppanen, M.S. Kurzer, A.S. Csallany, Nutr. Res. 23 (2003) 479.
[9] R.A. Dixon, C.L. Steel, Trends Plant Sci. 4 (1999) 394.
[10] C. Gerhauser, K. Klimo, E. Heiss, I. Neumann, A. Gamal-Eldeen, J. Knauft, G.Y. Liu, S. Sitthimonchai, N. Frank, Mutat. Res.—Fundam. Mol. Mech. Mutagen. 523 (2003) 163.
[11] R. Miksicek, J. Mol. Pharm. 44 (1993) 37.
[12] J.D.J. Kellis, L.E. Vickery, Science 225 (1984) 1032.
[13] L. Packer, G. Rimach, F. Virgili, Free Radic. Biol. Med. 27 (1999) 704.
[14] S.E. Nielsen, R. Freese, C. Cornett, L.O. Dragsted, Anal. Chem. 72 (2000) 1503.
[15] D. Romanová, D. Grandai, B. Jóková, P. Bodek, A. Vachálková, J. Chromatogr. A 870 (2000) 463.
[16] M. Careri, L. Elviri, A. Mangia, Rapid Commun. Mass Spectrom. 13 (1999) 2399.
[17] C.J. van Platerink, T.P.J. Mulder, P.J.W. Schuyl, J.M.M. van Amelsvoort, Proceedings of 48th ASMS Conference on Mass Spectrometry and Allied Topics, Long Beach, CA, 2000.
[18] X.-G. He, L.-Z. Lian, L.-Z. Lin, M.W. Bernart, J. Chromatogr. A 791 (1997) 127.
[19] N. Chaves, J.J. Ríos, C. Gutierrez, J.C. Escudero, J.M. Olías, J. Chromatogr. A 799 (1998) 111.
[20] X. He, L. Lin, L. Lian, J. Chromatogr. A 755 (1996) 127.
[21] P. Bednarek, L. Kerhoas, P. Wojtaszek, J. Einhorn, M. Stobiecki, Proceedings of 15th International Mass Spectrometry Conference, Barcelona, Spain, 27 August–1 September 2000.
[22] Y.-L. Ma, I. Vedernikova, H. Van den Heuvel, M. Claeys, J. Am. Soc. Mass Spectrom. 11 (2000) 136.
[23] B.J. Boersma, R.P. Patel, M. Kirk, P.L. Jackson, D. Muccio, V.M. Darley-Usmar, S. Barnes, Arch. Biochem. Biophys. 368 (1999) 265.
[24] R. Franski, W. Bylka, I. Matlawska, M. Stobiecki, Proceedings of 15th International Mass Spectrometry Conference, Barcelona, Spain, 27 August–1 September 2000.
[25] F. Cuyckens, Y.-L. Ma, H. Van den Heuvel, M. Claeys, Proceedings of 15th International Mass Spectrometry Conference, Barcelona, Spain, 27 August–1 September 2000.
[26] M.A. Almoster-Ferreira, P. Esperança, M.C. Oliviera, Proceedings of 15th International Mass Spectrometry Conference, Barcelona, Spain, 27 August–1 September 2000.
[27] C. Cren-Olivé, S. Deprez, B. Coddeville, C. Rolando, Proceedings of 15th International Mass Spectrometry Conference, Barcelona, Spain, 27 August–1 September 2000.
[28] M.T. Fernandez, M.L. Mira, M.H. Florêncio, K.R. Jennings, Proceedings of 15th International Mass Spectrometry Conference, Barcelona, Spain, 27 August–1 September 2000.
[29] C. Borges, P. Martinho, A. Martins, A.P. Rauter, M.A. Almoster Ferreira, Rapid Commun. Mass Spectrom. 15 (2001) 1760.
[30] Y.Y. Lin, K.J. Ng, J. Kwokei, S. Yang, J. Chromatogr. 629 (1993) 389.
[31] M.S. Lee, D.J. Hook, E.H. Kerns, K.J. Volk, I.E. Rosenberg, Biol. Mass Spectrom. 22 (1993) 84.
[32] M. Saegesser, M. Meinzer, J. Am. Soc. Brew. Chem. 54 (1996) 129.
[33] A. Raffaelli, G. Moneti, V. Mercati, E. Toja, J. Chromatogr. A 777 (1997) 223.
[34] S. Chimichi, V. Mercati, G. Moneti, A. Raffaelli, E. Toja, Nat. Prod. Lett. 11 (1998) 225.
[35] J.F. Stevens, A.W. Taylor, M.L. Deinzer, J. Chromatogr. A 832 (1/2) (1999) 97.
[36] B. Ameer, R.A. Weintraub, J.V. Johnson, R.A. Yost, R.L. Rouseff, Clin. Pharmacol. Ther. (St. Louis) 60 (1) (1996) 34.
[37] J.F. Stevens, E. Wollenweber, M. Ivancic, V.L. Hsu, S. Sundberg, M.L. Deinzer, Phytochemistry 51 (1999) 771.
[38] R.J. Hughes, T.R. Croley, C.D. Metcalfe, R.E. March, Int. J. Mass Spectrom. 210/211 (2001) 371.
[39] T.R. Croley, R.J. Hughes, C.D. Metcalfe, R.E. March, Rapid Commun. Mass Spectrom. 14 (2000) 1494.
[40] T.R. Croley, R.J. Hughes, C. Hao, C.D. Metcalfe, R.E. March, Rapid Commun. Mass Spectrom. 14 (2000) 2154.
[41] N. Fabre, I. Rustan, E. de Hoffmann, J. Quetin-Leclercq, J. Am. Soc. Mass Spectrom. 12 (2001) 707.
[42] F. Cuyckens, R. Rozenberg, E. de Hoffmann, M. Claeys, J. Mass Spectrom. 36 (2001) 1203.

[43] Y.-L. Ma, F. Cuyckens, H. Van den Heuvel, M. Claeys, Phytochem. Anal. 12 (2001) 159.
[44] R.A. Dixon, N.L. Paiva, The Plant Cell 7 (1995) 1085.
[45] R.E. March, X.-S. Miao, Int. J. Mass Spectrom. 231 (2004) 157.
[46] T.J. Mabry, K.R. Markham, in: J.B. Harborne, T.J. Mabry, H. Mabry (Eds.), The Flavonoids, Academic Press, New York, 1975, p. 78.
[47] A. Baracco, G. Bertin, E. Gnocco, M. Legorati, S. Sedocco, S. Catinella, D. Favretto, P. Traldi, Rapid Commun. Mass Spectrom. 9 (1995) 427.
[48] C.G. de Koster, W. Heerma, G. Dijkstra, G.J. Niemann, Biomed. Mass Spectrom. 12 (1985) 596.
[49] Y.L. Ma, Q.M. Li, H. Van den Heuvel, M. Claeys, Rapid Commun. Mass Spectrom. 11 (1997) 1357.
[50] B. Domon, C. Costello, Glycoconjugate J. 5 (1988) 397.
[51] Q.M. Li, M. Claeys, Biol. Mass Spectrom. 23 (1994) 406.
[52] E. Hvattum, Rapid Commun. Mass Spectrom. 16 (2002) 655.
[53] E. Hvattum, D. Ekeberg, J. Mass Spectrom. 38 (2003) 43.
[54] R.E. March, X.-S. Miao, C.D. Metcalfe, M. Stobiecki, I. Matlawska, W. Bylka, Proceedings of 16th International Mass Spectrometry Conference, Edinburgh, 31 August–5 September 2003.
[55] R.E. March, E.G. Lewars, C. Stadey, X.-S. Miao, C.D. Metcalfe, M. Stobiecki, L. Marczak, Proceedings of 16th Tandem Mass Spectrometry Workshop, Lake Louise, Alberta, Canada, 3–6 December 2003.